

# Recognition of RNA duplexes by chemically modified triplex-forming oligonucleotides

Zhou, Y.; Kierzek, E.; Loo, Z. P.; Antonio, M.; Yau, Yin Hoe; Chuah, Y. W.; Geifman-Shochat, Susana; Kierzek, R.; Chen, Gang

2013

Zhou, Y., Kierzek, E., Loo, Z. P., Antonio, M., Yau, Y. H., Chuah, Y. W., Geifman-Shochat, S., Kierzek, R., & Chen, G. (2013). Recognition of RNA duplexes by chemically modified triplex-forming oligonucleotides. *Nucleic Acids Research*, 41(13), 6664-6673.

<https://hdl.handle.net/10356/98149>

<https://doi.org/10.1093/nar/gkt352>

---

© 2013 The Author(s). Published by Oxford University Press. This is an Open Access article distributed under the terms of the Creative Commons Attribution License (<http://creativecommons.org/licenses/by/3.0/>), which permits unrestricted reuse, distribution, and reproduction in any medium, provided the original work is properly cited.

*Downloaded on 23 Aug 2022 04:13:12 SGT*

# Recognition of RNA duplexes by chemically modified triplex-forming oligonucleotides

Yuan Zhou<sup>1</sup>, Elzbieta Kierzek<sup>2</sup>, Zi Ping Loo<sup>1</sup>, Meraldo Antonio<sup>1</sup>, Yin Hoe Yau<sup>3</sup>, York Wiew Chuan<sup>3</sup>, Susana Geifman-Shochat<sup>3</sup>, Ryszard Kierzek<sup>2,\*</sup> and Gang Chen<sup>1,\*</sup>

<sup>1</sup>Division of Chemistry and Biological Chemistry, School of Physical and Mathematical Sciences, Nanyang Technological University, 21 Nanyang Link, Singapore 637371, <sup>2</sup>Institute of Bioorganic Chemistry, Polish Academy of Sciences, Noskowskiego 12/14, 61-704 Poznan, Poland and <sup>3</sup>Division of Structural Biology and Biochemistry, School of Biological Sciences, Nanyang Technological University, 60 Nanyang Drive, Singapore 637551

Received October 8, 2012; Revised April 10, 2013; Accepted April 12, 2013

## ABSTRACT

Triplex is emerging as an important RNA tertiary structure motif, in which consecutive non-canonical base pairs form between a duplex and a third strand. RNA duplex region is also often functionally important site for protein binding. Thus, triplex-forming oligonucleotides (TFOs) may be developed to regulate various biological functions involving RNA, such as viral ribosomal frameshifting and reverse transcription. How chemical modification in TFOs affects RNA triplex stability, however, is not well understood. Here, we incorporated locked nucleic acid, 2-thio U- and 2'-O methyl-modified residues in a series of all pyrimidine RNA TFOs, and we studied the binding to two RNA hairpin structures. The 12-base-triple major-groove pyrimidine-purine-pyrimidine triplex structures form between the duplex regions of RNA/DNA hairpins and the complementary RNA TFOs. Ultraviolet-absorbance-detected thermal melting studies reveal that the locked nucleic acid and 2-thio U modifications in TFOs strongly enhance triplex formation with both parental RNA and DNA duplex regions. In addition, we found that incorporation of 2'-O methyl-modified residues in a TFO destabilizes and stabilizes triplex formation with RNA and DNA duplex regions, respectively. The (de)stabilization of RNA triplex formation may be facilitated through modulation of van der Waals contact, base stacking, hydrogen bonding, backbone pre-organization, geometric compatibility and/or dehydration energy. Better understanding of the molecular determinants of RNA triplex structure stability lays the foundation for designing and

discovering novel sequence-specific duplex-binding ligands as diagnostic and therapeutic agents targeting RNA.

## INTRODUCTION

The biological functions of RNAs include gene regulation, catalysis, immunomodulation and acting as templates for the synthesis of protein, RNA and DNA. Recent advances in understanding the structures, energetics and functions of RNAs provide the foundation for developing nucleic acid-based diagnostics, therapeutics and nanobiotechnologies (1–7). Triplex is emerging as an important RNA tertiary structure motif, in which consecutive non-canonical base pairs (see Figure 1A for example) form between a duplex and a third strand (8–18). RNA duplex region is also often functionally important site for protein binding (19–25). Thus, there is a great potential to design and discover chemically modified triplex-forming oligonucleotides (TFOs) and other therapeutic ligands targeting RNA duplex regions, via reprogramming of RNA–RNA and RNA–protein interactions.

Formation of major-groove pyrimidine-purine-pyrimidine triplexes with parental DNA duplexes (Figures 1 and 2) facilitates sequence-specific DNA cleavage (26,27) and inhibition of transcription (28). Thus, extensive studies have been carried out to use chemically modified TFOs to enhance the binding affinity with DNA duplexes (29,30). For example, 2'-O methyl (2'-OMe) (Figure 1B) modification in TFOs favors triplex formation (31,32) with parental DNA duplexes. Incorporation of locked nucleic acid (LNA) [also known as 2',4'-bridged nucleic acid (2',4'-BNA)] monomers (Figure 1B) significantly enhances triplex formation with DNA duplexes (33–35). A base modification, 2-thio U (Figure 1B) in TFOs, is effective in stabilization of triplexes with parental DNA duplexes (36).

\*To whom correspondence should be addressed. Tel: +65 6592 2549; Fax: +65 6791 1961; Email: RNACHEN@ntu.edu.sg  
Correspondence may also be addressed to Ryszard Kierzek. Tel: +48 61 852 85 03; Fax: +48 61 852 05 32; Email: rkierzek@ibch.poznan.pl

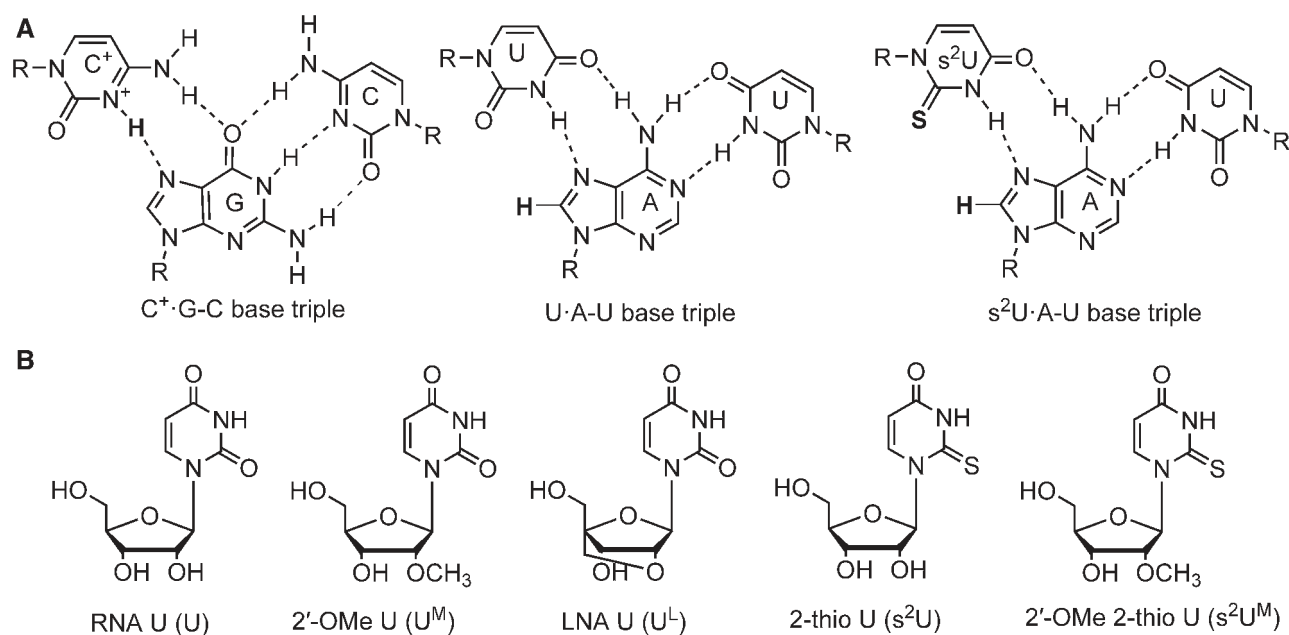


**Figure 1.** (A) Base triples studied in this article. The N3 atom of C base needs to be protonated (shown in bold) to form C<sup>+</sup>·G-C base triple. The s<sup>2</sup>U·A-U base triple is more stable than unmodified U·A-U base triple because of enhanced van der Waals interaction between the thio group in 2-thio U and H8 hydrogen (shown in bold) in A and other molecular interactions. (B) Chemical structures of nucleosides: RNA U (U), 2'-OMe U (U<sup>M</sup>), LNA U (U<sup>L</sup>), 2-thio U (s<sup>2</sup>U) and 2'-OMe 2-thio U (s<sup>2</sup>U<sup>M</sup>).

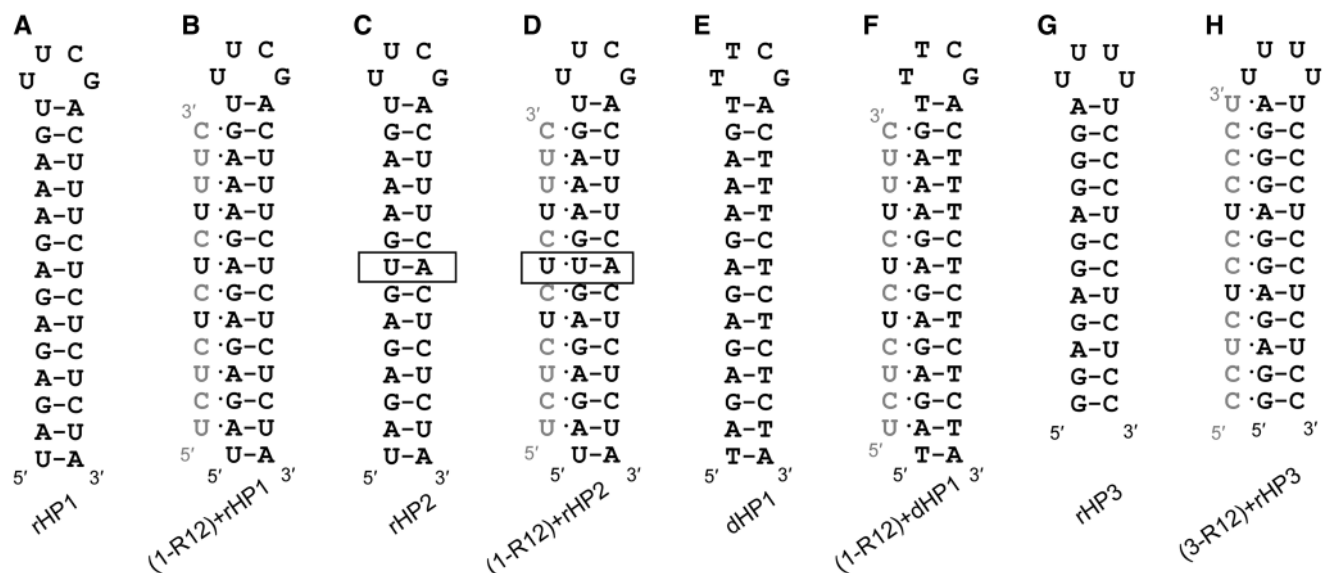


**Figure 2.** Hairpin and triplex structures studied in this article. Representative TFOs' strands (1-R12 or 3-R12) are shown in gray with the residues to be modified shown in black. (A) A 14-bp 32-nt RNA hairpin (rHP1). (B) A triplex formed between TFO 1-R12 and rHP1. (C) A mutated (U-A inversion, shown in box) 14-bp 32-nt RNA hairpin (rHP2). (D) A hypothetical triplex formed between non-complementary TFO 1-R12 and rHP2. A mismatched base triple (U·U-A) is indicated. (E) A 14-bp 32-nt DNA hairpin (dHP1), which is homologous to rHP1. (F) A triplex formed between TFO 1-R12 and dHP1. (G) A 12-bp 28-nt RNA hairpin (rHP3). (H) A triplex formed between TFO 3-R12 and rHP3.

Surprisingly, limited studies have been reported in targeting RNA duplex regions by triplex formation. To the best of our knowledge, it is not known how incorporation of LNA and 2-thio U-modified residues into TFOs affects RNA triplex stability. Here, we incorporated LNA U (U<sup>L</sup>), 2-thio U (s<sup>2</sup>U), 2'-OMe 2-thio U (s<sup>2</sup>U<sup>M</sup>), 2'-OMe

U (U<sup>M</sup>) and 2'-OMe C (C<sup>M</sup>) residues into 12-nt all pyrimidine RNA TFOs, and we studied the major-groove triplex formation of the modified TFOs with RNA and DNA hairpins (Figure 2) by ultraviolet (UV)-absorbance-detected thermal melting at various NaCl concentrations and pH's. The RNA triplex formation was further

tested by gel electrophoresis and surface plasmon resonance (SPR) experiments.

## MATERIALS AND METHODS

### Oligonucleotides

Chemically synthesized and purified DNA hairpin 1 (dHP1), RNA hairpin 1 (rHP1), RNA hairpin 2 (rHP2), RNA hairpin 3 (rHP3), biotin-labeled RNAs and unmodified RNA TFOs (Figure 2) were purchased from Sigma-Aldrich in Singapore. Chemically modified TFOs were chemically synthesized, deprotected and purified as reported (37–39). All oligonucleotides were characterized by electrospray ionization mass spectrometry (ESI-MS). The sequences of TFOs are listed in Table 1.

### UV-absorbance-detected thermal melting

All UV absorbance versus temperature thermal melting studies were carried out using a Beckman DU 800 spectrophotometer connected to a computer for data collection and analysis. High-performance transport and multiple-cell holder were used. The temperature was increased from 15 to 95°C and then decreased back to 15°C at a ramp rate of 0.2°C/min (or 1°C/min for duplexes formed between TFO strands and a 12-nt all purine strand, 5'-AGAGAGAGAAAG-3') with a Peltier temperature controller, and the absorbance at 260 or 265 nm (only for 1-Rs<sup>2</sup>U3) was recorded every 0.5°C. The samples for UV-absorbance-detected thermal melting studies contained 5 μM hairpin and 5 μM TFO in 100–1000 mM NaCl, 0.5 mM ethylenediaminetetraacetic acid (EDTA), 20 mM 2-morpholinoethanesulfonic acid (MES) (pH 5.0, 5.5 and 6.0) or 20 mM 4-(2-Hydroxyethyl)piperazine-1-ethanesulfonic acid

(HEPES) (pH 6.5, 6.8 and 7.0). We chose MES and HEPES buffers because their pK<sub>a</sub> values are relatively independent of temperature (40). A detailed triplex annealing protocol can be found in the Supplementary Data. The first derivative curves were fit to Gaussian functions, and the temperatures with maximum first derivatives (at Gaussian peaks) in the melting (heating) curves were taken as the melting temperatures (*T*<sub>m1</sub> for triplex to hairpin transition and *T*<sub>m2</sub> for hairpin to single-strand transition). Hysteresis between heating and cooling curves was observed for triplex to hairpin transitions. No hysteresis was observed for hairpin to single-strand transition. Equilibrium thermodynamic parameters for the triplex to hairpin transitions were not obtained because of the hysteresis. Equilibrium thermodynamic parameters for the duplex and hairpin formation were obtained by fitting to a two-state model with the MeltWin program (41).

### Gel electrophoresis

The native polyacrylamide gel electrophoresis experiments were performed in 16.5 × 22-cm gel containing 12% acrylamide (acrylamide/Bis-acrylamide = 19:1) at 4°C. RNA hairpin and TFOs were both 1 μM, which were incubated in 40 μl of buffer of 100 mM NaCl, 20 mM MES and 0.5 mM EDTA at pH 5.5, and left for 3 h before loading. Eight microliters of 35% glycerol was then added into 40 μl of loading buffer. The running buffer contains 10 mM NaCl, 2 mM MgCl<sub>2</sub> and 1 × TAE (40 mM Tris-acetate and 1 mM EDTA) at pH 6. The gel electrophoresis experiments were run at 160 V for 12–16 h, and the gels were stained by ethidium bromide, and the hairpin and triplex bands were imaged by a Typhoon scanner (GE Healthcare).

**Table 1.** TFO sequences studied in this article

TFO	Sequence (5'-3') <sup>a</sup>											
1-D12 <sup>b</sup>	T	C	T	C	T	C	T	C	T	T	T	C
1-R12	U	C	U	C	U	C	U	C	U	U	U	C
Control	A	U	C	U	G	U	U	C	C	A	C	U
1-RU <sup>L</sup> 1	U	C	U	C	U	C	U <sup>L</sup>	C	C	U	U	C
1-RU <sup>L</sup> 2	U	C	U	C	U <sup>L</sup>	C	U <sup>L</sup>	C	U	U	U	C
1-RU <sup>L</sup> 3	U	C	U	C	U <sup>L</sup>	C	U <sup>L</sup>	C	U <sup>L</sup>	U	U	C
1-Rs <sup>2</sup> U1	U	C	U	C	U	C	s <sup>2</sup> U	C	U	U	U	C
1-Rs <sup>2</sup> U2	U	C	U	C	s <sup>2</sup> U	C	s <sup>2</sup> U	C	U	U	U	C
1-Rs <sup>2</sup> U3	U	C	U	C	s <sup>2</sup> U	C	s <sup>2</sup> U	C	s <sup>2</sup> U	U	U	C
1-RU <sup>M</sup> 3	U	C	U	C	U <sup>M</sup>	C	U <sup>M</sup>	C	U <sup>M</sup>	U	U	C
1-M12	U <sup>M</sup>	C <sup>M</sup>	U <sup>M</sup>	C <sup>M</sup>	U <sup>M</sup>	C <sup>M</sup>	U <sup>M</sup>	C <sup>M</sup>	U <sup>M</sup>	U <sup>M</sup>	U <sup>M</sup>	C <sup>M</sup>
1-MU <sup>L</sup> 1	U <sup>M</sup>	C <sup>M</sup>	U <sup>M</sup>	C <sup>M</sup>	U <sup>M</sup>	C <sup>M</sup>	U <sup>L</sup>	C <sup>M</sup>	U <sup>M</sup>	U <sup>M</sup>	U <sup>M</sup>	C <sup>M</sup>
1-MU <sup>L</sup> 2	U <sup>M</sup>	C <sup>M</sup>	U <sup>M</sup>	C <sup>M</sup>	U <sup>L</sup>	C <sup>M</sup>	U <sup>L</sup>	C <sup>M</sup>	U <sup>M</sup>	U <sup>M</sup>	U <sup>M</sup>	C <sup>M</sup>
1-MU <sup>L</sup> 3	U <sup>M</sup>	C <sup>M</sup>	U <sup>M</sup>	C <sup>M</sup>	U <sup>L</sup>	C <sup>M</sup>	U <sup>L</sup>	C <sup>M</sup>	U <sup>L</sup>	U <sup>M</sup>	U <sup>M</sup>	C <sup>M</sup>
1-Ms <sup>2</sup> U <sup>M</sup> 1	U <sup>M</sup>	C <sup>M</sup>	U <sup>M</sup>	C <sup>M</sup>	U <sup>M</sup>	C <sup>M</sup>	s <sup>2</sup> U <sup>M</sup>	C <sup>M</sup>	U <sup>M</sup>	U <sup>M</sup>	U <sup>M</sup>	C <sup>M</sup>
1-Ms <sup>2</sup> U <sup>M</sup> 2	U <sup>M</sup>	C <sup>M</sup>	U <sup>M</sup>	C <sup>M</sup>	s <sup>2</sup> U <sup>M</sup>	C <sup>M</sup>	s <sup>2</sup> U <sup>M</sup>	C <sup>M</sup>	U <sup>M</sup>	U <sup>M</sup>	U <sup>M</sup>	C <sup>M</sup>
1-Ms <sup>2</sup> U <sup>M</sup> 3	U <sup>M</sup>	C <sup>M</sup>	U <sup>M</sup>	C <sup>M</sup>	s <sup>2</sup> U <sup>M</sup>	C <sup>M</sup>	s <sup>2</sup> U <sup>M</sup>	C <sup>M</sup>	s <sup>2</sup> U <sup>M</sup>	U <sup>M</sup>	U <sup>M</sup>	C <sup>M</sup>
3-R12	C	C	U	C	U	C	C	U	C	C	C	U
3-Rs <sup>2</sup> U2	C	C	U	C	s <sup>2</sup> U	C	C	s <sup>2</sup> U	C	C	C	U
3-RU <sup>L</sup> 2	C	C	U	C	U <sup>L</sup>	C	C	U <sup>L</sup>	C	C	C	U

<sup>a</sup>All listed sequences have RNA residues unless otherwise noted. The modified nucleotides studied are LNA U (U<sup>L</sup>), 2-thio U (s<sup>2</sup>U), 2'-OMe U (U<sup>M</sup>), 2'-OMe C (C<sup>M</sup>) and 2'-OMe 2-thio U (s<sup>2</sup>U<sup>M</sup>). In the nomenclature for TFOs, the first number (1 or 3) indicates the TFO's complementary hairpin sequence (rHP1, dHP1 or rHP3), and the last number (1, 2, 3 or 12) indicates the number of modified residues. The first letters (D, R and M) indicate the main backbone compositions of DNA, RNA and 2'-OMe RNA, respectively.

<sup>b</sup>In TFO 1-D12, all 12 residues are unmodified deoxyribonucleotides.

## Surface plasmon resonance assay

All SPR experiments were run with a constant flow (10  $\mu$ l/min) of running buffer (100 mM NaCl, 0.5 mM EDTA and 20 mM MES, pH 5.5) on a Biacore T200 (BIAcore AB, GE Healthcare) with a carboxymethylated dextran-coated sensor chip (CM5-S) at 25°C. The surfaces were first activated for 7 min with 1:1 mixture of 0.2 M *N*-ethyl-*N'*-[3-(diethylamino)propyl]carbodiimide and 50 mM *N*-hydroxysuccinimide. Neutravidin was then dissolved into 10 mM sodium acetate at pH 6.0 and immobilized at 10  $\mu$ l/min flow rate onto the surfaces by standard amine coupling procedure to achieve 4000 RU. The surfaces were finally blocked with 0.5 M ethanolamine-HCl at pH 8.5 for 7 min. Biotinylated RNA hairpin (5'-biotin-TTT TGGAGAGGAGGGAUUUUCCCUCCUCUCC, with four DNA thymine (T) residues incorporated as a linker between biotin and RNA hairpin, rHP3) and an RNA hairpin control (5'-biotin-TTTTUAGAGAGAGAAAGU UUCGACUUUCUCUCUCUA, with four DNA thymine (T) residues incorporated as a linker between biotin and RNA hairpin, rHP1) were captured on sensor chip surfaces to  $\sim$ 740 RU. Serially diluted TFOs (3-R12, 3-Rs<sup>2</sup>U2, and 3-RU<sup>L</sup>2 at 82 nM, 247 nM, 741 nM, 2.2  $\mu$ M, 6.7  $\mu$ M and 20  $\mu$ M) were injected (10  $\mu$ l/min) for 10 min across the surfaces with immobilized RNA hairpins. After a dissociation period (1200 s), a 60 s pulse of 0.1% sodium dodecyl sulfate in H<sub>2</sub>O was applied to regenerate the surfaces, followed by a 10-min running buffer flow. All the sensorgrams were corrected by subtraction of the buffer blanks and responses of TFOs on the RNA hairpin control surface. Processed data were globally analyzed and fit to a simple 1:1 interaction model with mass transport coefficient.

## RESULTS AND DISCUSSION

### Effect of pH on RNA triplex formation

Cytosine N3 atoms in a TFO need to be protonated to form hydrogen bonds (Hoogsteen base pairs) with guanine N7 atoms in the purine strand of a duplex (Figures 1 and 2). Thus, we investigated the effect of pH on triplex formation. Our thermal melting studies for RNA triplexes formed between TFOs and RNA hairpins rHP1 and rHP3 (Figure 2A and G) reveal that the melting temperatures of the RNA hairpins ( $T_{m2}$ ) do not change significantly with pH (Figure 3A and B and Supplementary Table S1), consistent with previous studies for RNA duplex structures (42). The melting temperatures of the RNA triplexes ( $T_{m1}$ ) decrease significantly (by  $>20^\circ\text{C}$ ) with increasing pH (from pH 5.5 to 7.0) (Figure 3A–C and Supplementary Table S1), which is consistent with a  $pK_a$  of  $\sim$ 7.0 for cytosine N3 atoms in TFOs of major-groove RNA triplexes (9). Because of the hysteresis observed in triplex to hairpin transitions (see Supplementary Figure S3 for example), we did not obtain equilibrium thermodynamic parameters.

### Effect of salt concentration on RNA triplex formation

With increasing concentration of NaCl from 100 mM to 1 M, the melting temperature of the RNA hairpin ( $T_{m2}$ )

increases as expected, whereas the melting temperatures of the RNA triplexes ( $T_{m1}$ ) decrease modestly (Figure 3D–F and Supplementary Table S1). Destabilization of triplexes with increasing concentration of NaCl is probably because of the fact that increasing concentration of NaCl decreases the  $pK_a$  of N3 of cytosines in the TFOs, which in turn destabilizes the RNA triplexes at pH 5.0–7.0. Our results are consistent with the previous finding that Na<sup>+</sup> and H<sup>+</sup> are competitive in binding to unmodified DNA triplexes containing both C<sup>+</sup>•G–C and T•A–T base triples (43–45). Because of the fact that formation of C<sup>+</sup>•G–C base triples results in the release of Na<sup>+</sup>, a stronger salt-dependent triplex thermal stability is observed for rHP3 (eight G–C pairs, Figure 2B) than for rHP1 (five G–C pairs, Figure 2H) (Figure 3F). The pH and salt dependence measurements facilitate the interpretation of the chemical modification results (see later in the text).

### Incorporation of LNA U and 2-thio U in a TFO enhances its binding to an RNA duplex region

LNA modification (Figure 1B) pre-organizes oligonucleotides in an A-form-like structure by locking the sugar pucker in C3'-endo conformation and thus favors the formation of duplexes with complementary single-strand DNA or RNA and the formation of triplexes with parental DNA duplexes (33–35,38,46,47). It is known that C3'-endo sugar pucker in TFOs is favored in both RNA and DNA triplex formation (14,15,48–50). But how LNA incorporation in TFOs affects binding to an RNA duplex region is not known. Our thermal melting results (Figure 4A and Supplementary Table S1) reveal that LNA U-modified RNA TFOs enhance triplex thermal stability with parental RNA duplex structure segment within a hairpin (rHP1, Figure 2A). Triplexes with more uridines modified are more stable than those with less uridines modified (Figure 4A and Supplementary Table S1). The  $T_{m1}$  for the triplex with unmodified RNA TFO (1-R12) is 28.1°C in 200 mM NaCl at pH 6.0. At the same buffer condition, the  $T_{m1}$ 's for the triplexes with modified TFOs with one, two and three LNA U residues (1-RU<sup>L</sup>1, 1-RU<sup>L</sup>2 and 1-RU<sup>L</sup>3) are 36.5, 45.4 and 52.9°C, respectively. Similar stabilizing effect is observed for the complementary TFO (3-RU<sup>L</sup>2 versus 3-R12) binding to rHP3 (Figure 4B). rHP3 is only partially melted at  $\sim$ 90°C, consistent with previously reported results (51,52).

Each LNA modification increases  $T_{m1}$  by  $\sim$ 9°C (Figure 4A and B). Thus, stabilization effect of LNA incorporation is relatively position and sequence environment independent. We note that LNA modification disrupts a potential hydrogen bond between 2'-OH in the TFO and a non-bridging oxygen in the purine strand of a duplex (Figure 5) (14,15,48,53,54). The importance of this hydrogen bond is corroborated by the fact that a DNA TFO (1-D12, Table 1) does not bind to rHP1 (Supplementary Figure S1A), consistent with previous results (51,55). Thus, the energy penalty because of the loss of the hydrogen bonds is compensated by the pre-organization of TFO backbone. Thus, our results suggest that LNA may be incorporated into TFOs to enhance binding to RNA duplex regions.

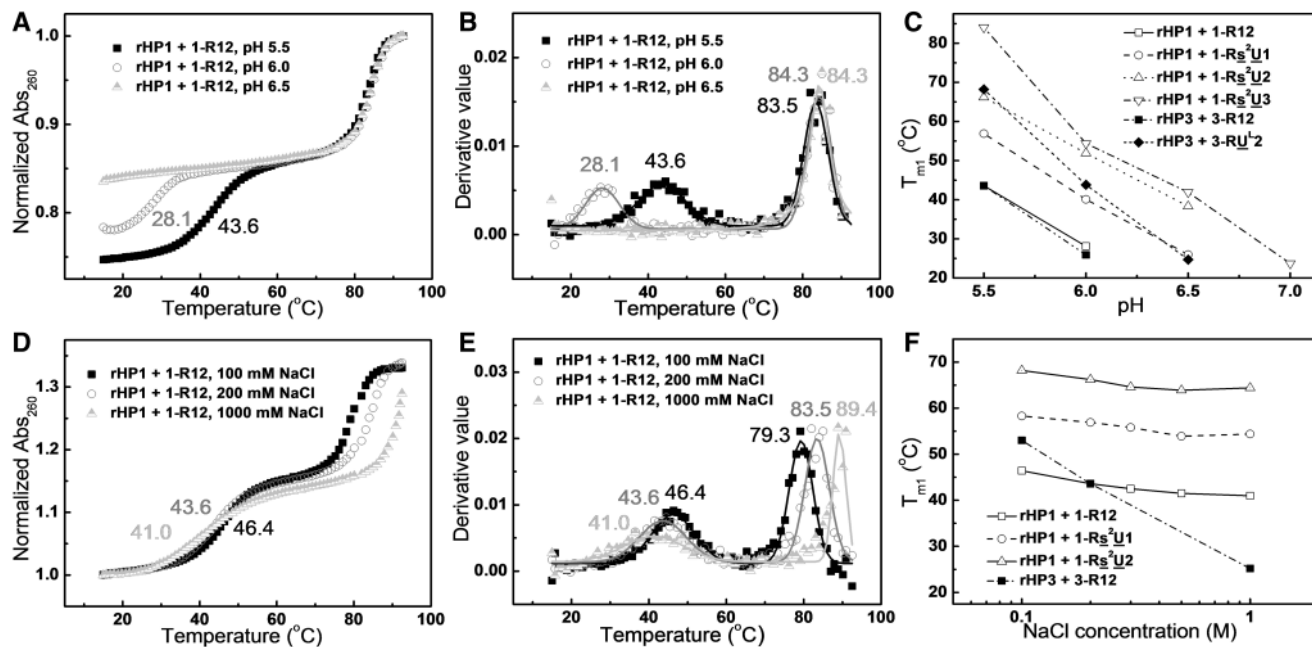


**Figure 3.** Effects of pH and NaCl concentration on RNA triplex thermal stability. (A) UV-absorbance-detected thermal melting curves of TFO 1-R12 binding to the RNA hairpin (rHP1, Figure 2A) at pH 5.5, 6.0 and 6.5 in 200 mM NaCl. (B) First derivatives of thermal melting curves in (A) reveal  $T_{m1}$  values of 43.6, 28.1 and  $<20^\circ\text{C}$ , respectively, at pH 5.5, 6.0 and 6.5. (C) Melting temperatures of triplexes ( $T_{m1}$ ) at various pH's in 200 mM NaCl. (D) Thermal melting curves of TFO 1-R12 binding to rHP1 at pH 5.5 in varying NaCl concentrations. (E) First derivatives of thermal melting curves in (D). With increasing NaCl concentration, triplex melting temperature ( $T_{m1}$ ) decreases, whereas hairpin (rHP1) melting temperature ( $T_{m2}$ ) increases. (F) Melting temperatures of triplexes ( $T_{m1}$ ) at pH 5.5 in different NaCl concentrations.

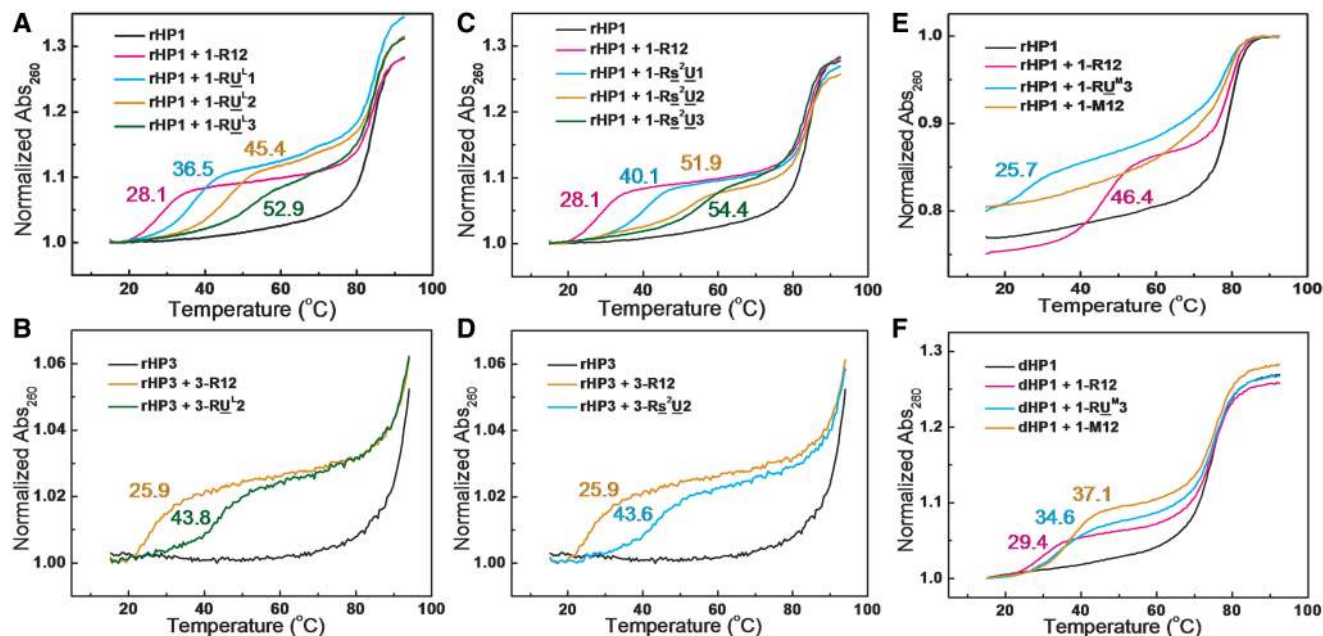


**Figure 4.** Effects of TFO base and sugar modifications on RNA triplex thermal stability in 200 mM NaCl at pH 6.0 unless otherwise noted. (A and B) UV-absorbance-detected thermal melting curves of LNA-modified TFOs binding to rHP1 and rHP3. First derivatives of thermal melting curves reveal  $T_{m1}$  values of 28.1, 36.5, 45.4 and  $52.9^\circ\text{C}$ , respectively, for 1-R12, 1-RU<sup>1</sup>, 1-RU<sup>2</sup> and 1-RU<sup>3</sup>.  $T_{m1}$  values are 25.9 and  $43.8^\circ\text{C}$ , respectively, for 3-R12 and 3-RU<sup>2</sup> binding to rHP3. (C and D) The 2-thio U-modified TFOs binding to rHP1. The absorption wavelength for 1-Rs<sup>2</sup>U3 binding to rHP1 was taken at 265 nm.  $T_{m1}$  values are 28.1, 40.1, 51.9 and  $54.4^\circ\text{C}$ , respectively, for 1-R12, 1-Rs<sup>2</sup>U1, 1-Rs<sup>2</sup>U2 and 1-Rs<sup>2</sup>U3.  $T_{m1}$  values are 25.9 and  $43.6^\circ\text{C}$ , respectively, for 3-R12 and 3-Rs<sup>2</sup>U2 binding to rHP3. (E) Incorporation of 2'-OMe residues in TFOs destabilizes (RNA)<sub>2</sub>-(TFO) triplex formation. The 2'-OMe-modified TFOs binding to rHP1 in 100 mM NaCl at pH 5.5.  $T_{m1}$  values are 46.4, 25.7 and  $<20^\circ\text{C}$ , respectively, for 1-R12, 1-RU<sup>M3</sup> and 1-M12. (F) Incorporation of 2'-OMe residues in TFOs stabilize (DNA)<sub>2</sub>-(TFO) triplex formation. The 2'-OMe-modified TFOs binding to dHP1 in 200 mM NaCl at pH 6.5.  $T_{m1}$  values are 29.4, 34.6 and  $37.1^\circ\text{C}$ , respectively, for 1-R12, 1-RU<sup>M3</sup> and 1-M12.

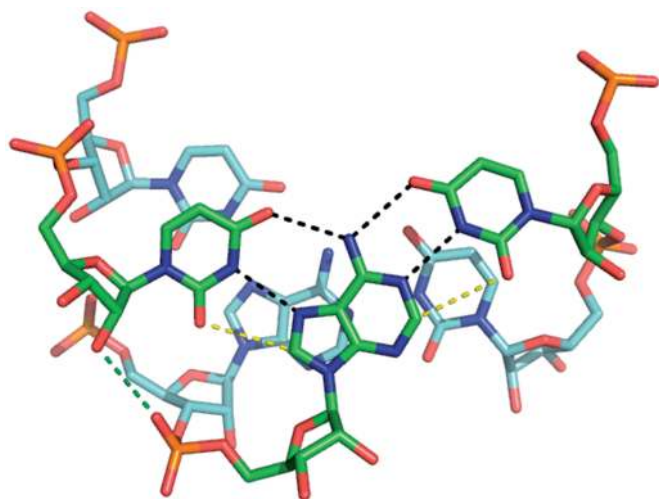


**Figure 5.** Stacking of two RNA U•A-U base triples (taken from PDB 3P22). Hydrogen bonds and van der Waals contacts (dashed lines) are shown only for the top base triple. The U•A-U base triple is stabilized by base-base hydrogen bonds (black dashed lines) and van der Waals contacts (yellow dashed lines and stacking interaction), all of which are enhanced by 2-thio U modification in the TFO strand. Base triples are also stabilized by hydrogen bonds between 2'-hydroxyl groups in the third strand and non-bridging oxygen in the purine strands of the RNA duplex (green dashed line). The 2'-OMe U modification in the third strand (TFO strand) disrupts this hydrogen bond, and the methyl group may cause steric clash with the backbone of the purine strand. LNA U modification in the TFO strand may not cause steric clash because of the fact that the methylene group is highly constrained.

The 2-thio U modification (Figure 1) in an oligonucleotide stabilizes the formation of RNA duplexes with complementary single-strand DNA or RNA and the formation of triplexes with a parental DNA duplex, respectively (36–38,49). Our thermal melting results reveal that incorporation of 2-thio U in a TFO also significantly stabilizes a triplex with a parental RNA duplex structure segment within a hairpin (rHP1, Figure 2A). The  $T_{m1}$ 's for the triplexes with one, two and three 2-thio U residues (1-Rs<sup>2</sup>U1, 1-Rs<sup>2</sup>U2 and 1-Rs<sup>2</sup>U3) in the TFOs are 40.1, 51.9 and 54.4°C, respectively, in 200 mM NaCl at pH 6.0 (Figure 4C and Supplementary Table S1). Similar stabilizing effect is also observed for the complementary TFO (3-Rs<sup>2</sup>U2 versus 3-R12) binding to rHP3 (Figure 4D).

The stabilization effect of 2-thio U modification in a TFO is probably because of the fact that the steric repulsion between the 2'-hydroxyl group of the ribose and the bulky 2-thio group of 2-thio U favors C3'-endo conformation of the ribose (56), which facilitates stable triplex formation (48). Base-base hydrogen bonding interaction (between the imino proton H3 in 2-thio U and N7 in A) is also enhanced with decreased  $pK_a$  of N3 (from 9.3 to 8.8) on thiolation of U (49,57). In addition, 2-thio U modification enhances TFO binding by reduced thermodynamic cost of dehydration and improved van der Waals contact between sulfur atom in 2-thio U and H8 hydrogen in A (Figures 1A and 5) (37,58).

Moreover, the enhanced triplex stability may be explained in terms of the strong stacking effect of the

2-thio group with adjacent bases (Figure 5) (36). Base-base stacking interactions are sequence environment dependent (42,43,59,60), which may explain one extra 2-thio U modification in 1-Rs<sup>2</sup>U3, which is flanked by C and U (Table 1), increases  $T_{m1}$  by only ~3°C relative to 1-Rs<sup>2</sup>U2 (Figure 4C). In contrast, the 2-thio U modifications present in 1-Rs<sup>2</sup>U1, 1-Rs<sup>2</sup>U2 and 3-Rs<sup>2</sup>U2 are all flanked by two C's, with each modification increasing  $T_{m1}$  by ~10°C (Figure 4C and D). The 2-thio U is a naturally occurring modification in RNA (61). Thus, nature may have evolved to use the conservative atomic mutation (2-thio U) to modulate RNA secondary and tertiary structure stability and function.

We confirmed triplex formation by native polyacrylamide gel electrophoresis experiment (Figure 6). The gels were post-stained by ethidium bromide, which intercalates into hairpin and triplex structures. As expected, the RNA hairpin bands moved faster than triplexes. In the lane 2 shown in Figure 6A and D, rHP1 and rHP3 were mixed with an RNA TFO control sequence (5'-AUCUGUCC ACU-3', Table 1), which is not sequence complementary to rHP1 or rHP3 to form triplexes. As expected, RNA triplex did not form between the RNA hairpins and RNA TFO control. Two bands were observed in lane 6 (Figure 6A) with a molar ratio of rHP1 to TFO (1-RU<sup>L</sup>1) at 1:0.5. The result suggests that a mixture of ~50% triplex and ~50% RNA hairpin is present in lane 6 (Figure 6A). Direct imaging of the all pyrimidine TFO bands by staining with Syber Green II was tested, but we observed only hairpin and triplex bands. Consistently, no apparent thermal melting transitions were observed for TFOs alone (data not shown). We did observe a band for an all purine 12-nt single-strand (5'-AG AGAGAGAAAG-3', Supplementary Figure S2C and D) by both ethidium bromide and Syber Green II staining (data not shown). Taken together, our thermal melting and gel results suggest that the designed RNA triplex structures (Figure 2B and H) form for unmodified RNA TFO and modified RNA TFOs incorporated with LNA U and 2-thio U residues. In addition, we carried out SPR experiment to monitor the triplex formation in real-time (Supplementary Figure S4). The SPR results suggest that the designed triplex structures (Figure 2H) indeed form.

### Binding specificity assay

We further tested the binding of the RNA TFOs to an RNA hairpin with one A-U base pair inverted compared with rHP1 (rHP2, Figure 2C and D). Our thermal melting results in 200 mM NaCl at varying pH reveal that the triplex melting temperatures ( $T_{m1}$ ) are <20°C at pH 6.0 (Supplementary Table S1). We tested TFOs 1-RU<sup>L</sup>1 and 1-Rs<sup>2</sup>U3 binding to rHP2 at low pH (5.5 and 5.0), and  $T_{m1}$  values were found to be >30°C lower than those of sequence-complementary triplexes when  $T_{m1}$  and  $T_{m2}$  are not overlapped (Supplementary Tables S1). The native gel results further confirm that triplexes do not form between rHP2 and TFOs with one mismatch (Supplementary Figure S1F-H). The results indicate that the TFOs have good sequence specificity in binding to an RNA duplex region.

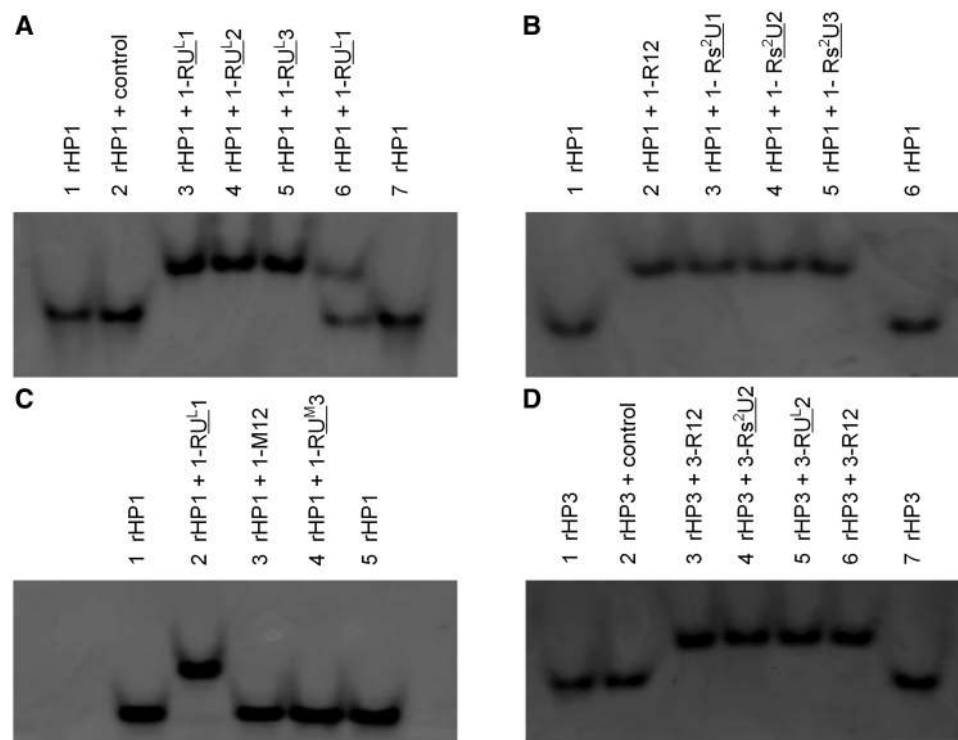


**Figure 6.** Native polyacrylamide gel for the RNA hairpins (rHP1 and rHP3) and triplexes. (A) rHP1 binds to modified RNA TFOs incorporated with LNA U residues. In lane 2, the control TFO (Table 1) does not bind to rHP1. In lane 6, rHP1 to 1-RU<sup>L</sup>-1 molar ratio is 1:0.5. The fact that only two bands (rHP1 and triplexes) were observed suggests that the designed RNA triplexes form without alternative structures. (B) rHP1 binds to unmodified and modified RNA TFOs incorporated with 2-thio U residues. (C) The 2'-OMe modifications in TFOs destabilize RNA triplex formation. RNA triplex bands were not observed for TFOs incorporated with three or more 2'-OMe residues. (D) rHP3 binds to unmodified and modified TFOs incorporated with 2-thio U and LNA U residues.

### Incorporation of 2'-OMe residues in a TFO destabilizes its binding to an RNA duplex region

We then investigated how 2'-OMe modification (Figure 1B) in a TFO affects the thermal stability of a triplex with a parental RNA duplex region (Figure 2B). The  $T_{m1}$  of triplex with TFO 1-RU<sup>M</sup>3 (25.7°C), which has three 2'-OMe residues, is lower than that with RNA TFO (1-R12) (46.4°C) in 100 mM NaCl at pH 5.5 (Figure 4E and Supplementary Table S1). All the complementary modified TFOs with more than three 2'-OMe modified residues do not bind to rHP1 (Figure 4E and Supplementary Table S1). No obvious gel electrophoresis mobility difference was seen between rHP1 alone and rHP1 mixed with TFOs with three or more 2'-OMe residues (Figure 6C and Supplementary Figure S1A and B), further suggesting that 2'-OMe TFOs do not bind to rHP1. The results indicate that 2'-OMe-modified TFOs destabilize triplex formation with RNA duplex region.

It is probable that substitution of 2'-OH with 2'-OMe disrupts the hydrogen bond between 2'-OH in the TFO and a non-bridging oxygen in the purine strand of a duplex (Figure 5) (14,15,48,53,54) and thus disfavors RNA triplex formation (32). In addition, unlike the highly restrained methylene group in LNA, the exposed methyl group in 2'-OMe RNA (Figure 1B) in the TFO may cause steric clash with the narrow major groove of the RNA duplex region.

### TFOs binding to a homologous DNA duplex region

Thermodynamically stable major-groove triplex structure formation without chemical modification is limited to a pyrimidine TFO strand binding to a duplex region with purines on one strand and pyrimidines on the other (50,62–64). Previous thermodynamic studies reveal that to form stable triplexes, RNA is preferred on both pyrimidine strands, whereas DNA is preferred on the purine strand (51). If the purine strand of a parental duplex region is RNA, only RNA TFO strand binds tightly to the parental duplex region (55).

To study the effect of target strand composition on triplex formation, we measured the binding of the complementary TFOs to a DNA hairpin target (dHP1, Figure 2E and F) with the same sequence as the RNA hairpin (rHP1, Figure 2A and B). Our thermal melting results reveal that the triplex melting temperatures ( $T_{m1}$ ) are always higher with a DNA duplex region than with a homologous RNA duplex region ( $\Delta T_{m1}$  ranging from 6 to 21°C in 200 mM NaCl at pH 6.0) (Supplementary Table S1). The DNA hairpin, dHP1, has a melting temperature ( $T_{m2}$ ) of ~74°C in 200 mM NaCl, which is ~10°C lower than the RNA hairpin, rHP1 (Figure 4, Supplementary Table S1), consistent with the prediction from nearest-neighbor models (59,65,66).

The relatively wider major groove of a DNA duplex (compared with an RNA duplex) may provide relatively



easier access for TFO binding. Consistently, incorporation of 2'-OMe residues in TFOs was found to enhance binding to the DNA hairpin, dHP1 (Figure 4F and Supplementary Table S1), which is in contrast to the significant destabilization effect observed in TFOs binding to the RNA hairpin, rHP1 (see earlier in the text, Figure 4E and Supplementary Table S1). It is likely that the major groove of a DNA duplex is more geometrically compatible for accommodating a 2'-OMe-modified TFO. The results suggest that rules for enhancing DNA triplex formation may not be applicable for RNA triplex formation. One may simply incorporate 2'-OMe or other relatively bulky residues in a TFO to selectively target a DNA duplex over a homologous RNA duplex region.

### The hairpin rHP1 forms without alternative structures

As evidenced by the strand concentration independent  $T_{m2}$  of rHP1 (Supplementary Table S3), the designed hairpin structure forms without appreciable bimolecular duplex (with an internal loop). It is likely that chemically modified TFOs may displace the pyrimidine segment of the parental RNA hairpin to form parallel or antiparallel duplex structure as shown in Supplementary Figure S2A and B. To test the possibility of the formation of such alternative structures because of strand invasion, we carried out thermal melting studies for the duplexes formed between a 12-nt all purine strand (5'-AGAGAG AGAAAG-3', Supplementary Figure S2C and D) and various TFOs. The results reveal that most of the duplex formation is relatively pH independent ( $\Delta T_m$  is within 3°C from pH 7.0 to 5.5) and have lower  $T_m$  than that of the parental RNA hairpin, rHP1 (Supplementary Figure S5 and Supplementary Tables S1 and S2). The pH independence of melting temperatures suggests that 12-bp parallel RNA duplex structures (formed between TFO sequences and an all purine strand, Supplementary Figure S2D) do not form because the stability of parallel DNA duplex is pH dependent (67). Thus, 9-bp antiparallel duplex structures form between the 12-nt all purine strand and TFOs (see Supplementary Figure S2C for example).

The fact that most of the  $T_m$  values of the 9-bp antiparallel duplexes (Supplementary Figure S2C) are in between  $T_{m1}$  and  $T_{m2}$  of triplexes (Supplementary Figure S5 and Supplementary Tables S1 and S2) suggests that neither parallel nor antiparallel duplex structure forms due to strand invasion of rHP1 (Supplementary Figure S2A and B). In addition, there are only two bands observed in native gels (Figure 6 and Supplementary Figure S1), further suggesting no appreciable alternative structures form (63). Thus, our designed 12-base-triple triplex structures (Figure 2B) form between rHP1 and complementary unmodified and modified RNA TFOs incorporated with LNA U and 2-thio U residues.

### CONCLUSION

In this study, we have found that both base and sugar modifications in TFOs may modulate the triplex formation targeting RNA duplex regions. We note that both sugar methylation and base thiolation are naturally

occurring RNA modifications. The effects of sugar modifications are probably sequence environment independent. The 2'-OMe sugar modification may be selected (by nature) to destabilize RNA base triple formation because of the loss of a hydrogen bond and steric clash. LNA sugar modification in TFOs stabilizes RNA triplex structures because of backbone pre-organization, despite the loss of a hydrogen bond. The 2-thio U base modification in TFOs stabilizes RNA triplex formation in a sequence environment-dependent manner, probably because of the combined effects of enhanced van der Waals contact, hydrogen bonding, base stacking, backbone pre-organization and reduced energy penalty of dehydration. A thio group may be selected (by nature) to enhance van der Waals interaction with the hydrogen atoms in a duplex major groove (H8 in adenine and guanine, H5 and H6 in uracil and cytosine) and other interactions, and thus favor RNA base triple and other tertiary structures. Our results provide useful insights into rational design of more potent and selective triplex-forming ligands targeting biologically important RNA duplex regions. Studies of other chemical modifications in bases and/or sugar-phosphate backbone and detailed sequence-dependent thermodynamic and kinetic characterizations are in progress.

### SUPPLEMENTARY DATA

Supplementary Data are available at NAR Online: Supplementary Tables 1–3, Supplementary Figures 1–6, Supplementary Method and Supplementary References [41,59].

### ACKNOWLEDGEMENTS

The authors thank Professors Tianhu Li, Anh Tuan Phan, Brendan P. Orner, Bengang Xing, Fangwei Shao and Dawei Zhang for sharing instruments.

### FUNDING

Start-up grant of Nanyang Technological University (NTU) (to G.C.); NTU internal grant (Singapore Ministry of Education Academic Research Fund Tier 1) (to G.C.); National Institutes of Health [1R03TW008739-01 to E.K. and D.H. Turner]; National Science Center [N N301 788 440 to E.K. and UMO-2011/03/B/NZ1/00576 and UMO-2011/03/B/ST5/01098 to R.K.]. Funding for open access charge: Start-up grant of Nanyang Technological University (NTU) (to G.C.).

*Conflict of interest statement.* None declared.

### REFERENCES

- Kole, R., Krainer, A.R. and Altman, S. (2012) RNA therapeutics: beyond RNA interference and antisense oligonucleotides. *Nat. Rev. Drug Discov.*, **11**, 125–140.
- Wesolowski, D., Tae, H.S., Gandotra, N., Llopis, P., Shen, N. and Altman, S. (2011) Basic peptide-morpholino oligomer conjugate

- that is very effective in killing bacteria by gene-specific and nonspecific modes. *Proc. Natl Acad. Sci. USA*, **108**, 16582–16587.
3. Guan,L.R. and Disney,M.D. (2012) Recent advances in developing small molecules targeting RNA. *ACS Chem. Biol.*, **7**, 73–86.
  4. Akinc,A., Zumbuehl,A., Goldberg,M., Leshchiner,E.S., Busini,V., Hossain,N., Bacallado,S.A., Nguyen,D.N., Fuller,J., Alvarez,R. *et al.* (2008) A combinatorial library of lipid-like materials for delivery of RNAi therapeutics. *Nat. Biotechnol.*, **26**, 561–569.
  5. Barczak,A.K., Gomez,J.E., Kaufmann,B.B., Hinson,E.R., Cosimi,L., Borowsky,M.L., Onderdonk,A.B., Stanley,S.A., Kaur,D., Bryant,K.F. *et al.* (2012) RNA signatures allow rapid identification of pathogens and antibiotic susceptibilities. *Proc. Natl Acad. Sci. USA*, **109**, 6217–6222.
  6. Zhang,X., Servos,M.R. and Liu,J. (2012) Instantaneous and quantitative functionalization of gold nanoparticles with thiolated DNA using a pH-assisted and surfactant-free route. *J. Am. Chem. Soc.*, **134**, 7266–7269.
  7. Jaeger,L. and Chworos,A. (2006) The architectonics of programmable RNA and DNA nanostructures. *Curr. Opin. Struct. Biol.*, **16**, 531–543.
  8. Chen,G., Chang,K.Y., Chou,M.Y., Bustamante,C. and Tinoco,I. Jr (2009) Triplex structures in an RNA pseudoknot enhance mechanical stability and increase efficiency of -1 ribosomal frameshifting. *Proc. Natl Acad. Sci. USA*, **106**, 12706–12711.
  9. Theimer,C.A., Blois,C.A. and Feigon,J. (2005) Structure of the human telomerase RNA pseudoknot reveals conserved tertiary interactions essential for function. *Mol. Cell*, **17**, 671–682.
  10. Kim,N.K., Zhang,Q., Zhou,J., Theimer,C.A., Peterson,R.D. and Feigon,J. (2008) Solution structure and dynamics of the wild-type pseudoknot of human telomerase RNA. *J. Mol. Biol.*, **384**, 1249–1261.
  11. Gilbert,S.D., Rambo,R.P., Van Tyne,D. and Batey,R.T. (2008) Structure of the SAM-II riboswitch bound to S-adenosylmethionine. *Nat. Struct. Mol. Biol.*, **15**, 177–182.
  12. Qiao,F. and Cech,T.R. (2008) Triple-helix structure in telomerase RNA contributes to catalysis. *Nat. Struct. Mol. Biol.*, **15**, 634–640.
  13. Liu,F. and Theimer,C.A. (2012) Telomerase activity is sensitive to subtle perturbations of the TLC1 pseudoknot 3' stem and tertiary structure. *J. Mol. Biol.*, **423**, 719–735.
  14. Mitton-Fry,R.M., DeGregorio,S.J., Wang,J., Steitz,T.A. and Steitz,J.A. (2010) Poly(A) tail recognition by a viral RNA element through assembly of a triple helix. *Science*, **330**, 1244–1247.
  15. Ulyanov,N.B. and James,T.L. (2010) RNA structural motifs that entail hydrogen bonds involving sugar-phosphate backbone atoms of RNA. *New J. Chem.*, **34**, 910–917.
  16. Leontis,N.B. and Westhof,E. (2003) Analysis of RNA motifs. *Curr. Opin. Struct. Biol.*, **13**, 300–308.
  17. Ogle,J.M., Brodersen,D.E., Clemons,W.M. Jr, Tarry,M.J., Carter,A.P. and Ramakrishnan,V. (2001) Recognition of cognate transfer RNA by the 30S ribosomal subunit. *Science*, **292**, 897–902.
  18. Demeshkina,N., Jenner,L., Westhof,E., Yusupov,M. and Yusupova,G. (2012) A new understanding of the decoding principle on the ribosome. *Nature*, **484**, 256–259.
  19. Puglisi,E.V. and Puglisi,J.D. (2011) Secondary structure of the HIV reverse transcription initiation complex by NMR. *J. Mol. Biol.*, **410**, 863–874.
  20. Levensgood,J.D., Rollins,C., Mishler,C.H., Johnson,C.A., Miner,G., Rajan,P., Znosko,B.M. and Tolbert,B.S. (2012) Solution structure of the HIV-1 exon splicing silencer 3. *J. Mol. Biol.*, **415**, 680–698.
  21. Runyon,S.T. and Puglisi,J.D. (2003) Design of a cyclic peptide that targets a viral RNA. *J. Am. Chem. Soc.*, **125**, 15704–15705.
  22. Battiste,J.L., Mao,H.Y., Rao,N.S., Tan,R.Y., Muhandiram,D.R., Kay,L.E., Frankel,A.D. and Williamson,J.R. (1996)  $\alpha$  helix-RNA major groove recognition in an HIV-1 Rev peptide RRE RNA complex. *Science*, **273**, 1547–1551.
  23. Wiedenheft,B., Sternberg,S.H. and Doudna,J.A. (2012) RNA-guided genetic silencing systems in bacteria and archaea. *Nature*, **482**, 331–338.
  24. Nallagatla,S.R., Toroney,R. and Bevilacqua,P.C. (2011) Regulation of innate immunity through RNA structure and the protein kinase PKR. *Curr. Opin. Struct. Biol.*, **21**, 119–127.
  25. Davidson,A., Leeper,T.C., Athanassiou,Z., Patora-Komisarska,K., Karn,J., Robinson,J.A. and Varani,G. (2009) Simultaneous recognition of HIV-1 TAR RNA bulge and loop sequences by cyclic peptide mimics of Tat protein. *Proc. Natl Acad. Sci. USA*, **106**, 11931–11936.
  26. Moser,H.E. and Dervan,P.B. (1987) Sequence-specific cleavage of double helical DNA by triple helix formation. *Science*, **238**, 645–650.
  27. Le Doan,T., Perrouault,L., Praseuth,D., Habhouh,N., Decout,J.L., Thuong,N.T., Lhomme,J. and Helene,C. (1987) Sequence-specific recognition, photocrosslinking and cleavage of the DNA double helix by an oligo-[ $\alpha$ ]-thymidylate covalently linked to an azidoproflavine derivative. *Nucleic Acids Res.*, **15**, 7749–7760.
  28. Morgan,A.R. and Wells,R.D. (1968) Specificity of the three-stranded complex formation between double-stranded DNA and single-stranded RNA containing repeating nucleotide sequences. *J. Mol. Biol.*, **37**, 63–80.
  29. Duca,M., Vekhoff,P., Oussedik,K., Halby,L. and Arimondo,P.B. (2008) The triple helix: 50 years later, the outcome. *Nucleic Acids Res.*, **36**, 5123–5138.
  30. Fox,K.R. and Brown,T. (2011) Formation of stable DNA triplexes. *Biochem. Soc. Trans.*, **39**, 629–634.
  31. Shimizu,M., Konishi,A., Shimada,Y., Inoue,H. and Ohtsuka,E. (1992) Oligo(2'-O-methyl)ribonucleotides: effective probes for duplex DNA. *FEBS Lett.*, **302**, 155–158.
  32. Wang,S. and Kool,E.T. (1995) Relative stabilities of triple helices composed of combinations of DNA, RNA and 2'-O-methyl-RNA backbones: chimeric circular oligonucleotides as probes. *Nucleic Acids Res.*, **23**, 1157–1164.
  33. Torigoe,H., Hari,Y., Sekiguchi,M., Obika,S. and Imanishi,T. (2001) 2'-O,4'-C-methylene bridged nucleic acid modification promotes pyrimidine motif triplex DNA formation at physiological pH: Thermodynamic and kinetic studies. *J. Biol. Chem.*, **276**, 2354–2360.
  34. Brunet,E., Alberti,P., Perrouault,L., Babu,R., Wengel,J. and Giovannangeli,C. (2005) Exploring cellular activity of locked nucleic acid-modified triplex-forming oligonucleotides and defining its molecular basis. *J. Biol. Chem.*, **280**, 20076–20085.
  35. Vester,B. and Wengel,J. (2004) LNA (Locked nucleic acid): high-affinity targeting of complementary RNA and DNA. *Biochemistry*, **43**, 13233–13241.
  36. Okamoto,I., Seio,K. and Sekine,M. (2006) Triplex forming ability of oligonucleotides containing 2'-O-methyl-2-thiouridine or 2-thiothymidine. *Bioorg. Med. Chem. Lett.*, **16**, 3334–3336.
  37. Testa,S.M., Disney,M.D., Turner,D.H. and Kierzek,R. (1999) Thermodynamics of RNA-RNA duplexes with 2- or 4-thiouridines: implications for antisense design and targeting a group I intron. *Biochemistry*, **38**, 16655–16662.
  38. Carlucci,M., Kierzek,E., Olejnik,A., Turner,D.H. and Kierzek,R. (2009) Chemical synthesis of LNA-2-thiouridine and its influence on stability and selectivity of oligonucleotide binding to RNA. *Biochemistry*, **48**, 10882–10893.
  39. Kierzek,E., Mathews,D.H., Ciesielska,A., Turner,D.H. and Kierzek,R. (2006) Nearest neighbor parameters for Watson-Crick complementary heteroduplexes formed between 2'-O-methyl RNA and RNA oligonucleotides. *Nucleic Acids Res.*, **34**, 3609–3614.
  40. Moody,E.M., Lecomte,J.T.J. and Bevilacqua,P.C. (2005) Linkage between proton binding and folding in RNA: a thermodynamic framework and its experimental application for investigating pK<sub>a</sub> shifting. *RNA*, **11**, 157–172.
  41. McDowell,J.A. and Turner,D.H. (1996) Investigation of the structural basis for thermodynamic stabilities of tandem GU mismatches: solution structure of (rGAGGUCUC)<sub>2</sub> by two-dimensional NMR and simulated annealing. *Biochemistry*, **35**, 14077–14089.
  42. Chen,G., Kennedy,S.D. and Turner,D.H. (2009) A CA<sup>+</sup> pair adjacent to a sheared GA or AA pair stabilizes size-symmetric RNA internal loops. *Biochemistry*, **48**, 5738–5752.

43. Soto, A.M., Loo, J. and Marky, L.A. (2002) Energetic contributions for the formation of TAT/TAT, TAT/CGC<sup>+</sup>, and CGC<sup>+</sup>/CGC<sup>+</sup> base triplet stacks. *J. Am. Chem. Soc.*, **124**, 14355–14363.
44. Lee, H.T., Arciniegas, S. and Marky, L.A. (2008) Unfolding thermodynamics of DNA pyrimidine triplexes with different molecularities. *J. Phys. Chem. B*, **112**, 4833–4840.
45. Sugimoto, N., Wu, P., Hara, H. and Kawamoto, Y. (2001) pH and cation effects on the properties of parallel pyrimidine motif DNA triplexes. *Biochemistry*, **40**, 9396–9405.
46. Kierzek, E., Ciesielska, A., Pasternak, K., Mathews, D.H., Turner, D.H. and Kierzek, R. (2005) The influence of locked nucleic acid residues on the thermodynamic properties of 2'-O-methyl RNA/RNA heteroduplexes. *Nucleic Acids Res.*, **33**, 5082–5093.
47. Kierzek, E., Pasternak, A., Pasternak, K., Gdaniec, Z., Yildirim, I., Turner, D.H. and Kierzek, R. (2009) Contributions of stacking, preorganization, and hydrogen bonding to the thermodynamic stability of duplexes between RNA and 2'-O-methyl RNA with locked nucleic acids. *Biochemistry*, **48**, 4377–4387.
48. Holland, J.A. and Hoffman, D.W. (1996) Structural features and stability of an RNA triple helix in solution. *Nucleic Acids Res.*, **24**, 2841–2848.
49. Kumar, R.K. and Davis, D.R. (1997) Synthesis and studies on the effect of 2-thiouridine and 4-thiouridine on sugar conformation and RNA duplex stability. *Nucleic Acids Res.*, **25**, 1272–1280.
50. Gotfredsen, C.H., Schultze, P. and Feigon, J. (1998) Solution structure of an intramolecular pyrimidine-purine-pyrimidine triplex containing an RNA third strand. *J. Am. Chem. Soc.*, **120**, 4281–4289.
51. Roberts, R.W. and Crothers, D.M. (1992) Stability and properties of double and triple helices: dramatic effects of RNA or DNA backbone composition. *Science*, **258**, 1463–1466.
52. Li, M., Zengeya, T. and Rozners, E. (2010) Short peptide nucleic acids bind strongly to homopurine tract of double helical RNA at pH 5.5. *J. Am. Chem. Soc.*, **132**, 8676–8681.
53. Escude, C., Francois, J.C., Sun, J.S., Ott, G., Sprinzl, M., Garestier, T. and Helene, C. (1993) Stability of triple helices containing RNA and DNA strands: experimental and molecular modeling studies. *Nucleic Acids Res.*, **21**, 5547–5553.
54. Wilds, C.J. and Damha, M.J. (1999) Duplex recognition by oligonucleotides containing 2'-deoxy-2'-fluoro-D-arabinose and 2'-deoxy-2'-fluoro-D-ribose. Intermolecular 2'-OH-phosphate contacts versus sugar puckering in the stabilization of triple-helical complexes. *Bioconjug. Chem.*, **10**, 299–305.
55. Han, H. and Dervan, P.B. (1993) Sequence-specific recognition of double helical RNA and RNA-DNA by triple helix formation. *Proc. Natl Acad. Sci. USA*, **90**, 3806–3810.
56. Yamamoto, Y., Yokoyama, S., Miyazawa, T., Watanabe, K. and Higuchi, S. (1983) NMR analyses on the molecular mechanism of the conformational rigidity of 2-thioribothymidine, a modified nucleoside in extreme thermophile transfer-RNAs. *FEBS Lett.*, **157**, 95–99.
57. Gilli, P., Pretto, L., Bertolasi, V. and Gilli, G. (2009) Predicting hydrogen-bond strengths from acid-base molecular properties. The pK<sub>a</sub> slide rule: toward the solution of a long-lasting problem. *Acc. Chem. Res.*, **42**, 33–44.
58. Siegfried, N.A., Kierzek, R. and Bevilacqua, P.C. (2010) Role of unsatisfied hydrogen bond acceptors in RNA energetics and specificity. *J. Am. Chem. Soc.*, **132**, 5342–5344.
59. Xia, T., SantaLucia, J. Jr, Burkard, M.E., Kierzek, R., Schroeder, S.J., Jiao, X., Cox, C. and Turner, D.H. (1998) Thermodynamic parameters for an expanded nearest-neighbor model for formation of RNA duplexes with Watson-Crick base pairs. *Biochemistry*, **37**, 14719–14735.
60. Chen, G., Kierzek, R., Yildirim, I., Krugh, T.R., Turner, D.H. and Kennedy, S.D. (2007) Stacking effects on local structure in RNA: changes in the structure of tandem GA pairs when flanking GC pairs are replaced by isoG-isoC pairs. *J. Phys. Chem. B*, **111**, 6718–6727.
61. Cantara, W.A., Crain, P.F., Rozenski, J., McCloskey, J.A., Harris, K.A., Zhang, X., Vendeix, F.A., Fabris, D. and Agris, P.F. (2011) The RNA modification database, RNAMDB: 2011 update. *Nucleic Acids Res.*, **39**, D195–D201.
62. Plum, G.E., Pilch, D.S., Singleton, S.F. and Breslauer, K.J. (1995) Nucleic acid hybridization: triplex stability and energetics. *Annu. Rev. Biophys. Biomol. Struct.*, **24**, 319–350.
63. Blose, J.M., Silverman, S.K. and Bevilacqua, P.C. (2007) A simple molecular model for thermophilic adaptation of functional nucleic acids. *Biochemistry*, **46**, 4232–4240.
64. Radhakrishnan, I. and Patel, D.J. (1994) DNA triplexes: solution structures, hydration sites, energetics, interactions, and function. *Biochemistry*, **33**, 11405–11416.
65. Mathews, D.H., Disney, M.D., Childs, J.L., Schroeder, S.J., Zuker, M. and Turner, D.H. (2004) Incorporating chemical modification constraints into a dynamic programming algorithm for prediction of RNA secondary structure. *Proc. Natl Acad. Sci. USA*, **101**, 7287–7292.
66. SantaLucia, J. Jr and Hicks, D. (2004) The thermodynamics of DNA structural motifs. *Annu. Rev. Biophys. Biomol. Struct.*, **33**, 415–440.
67. Ohmichi, T., Kawamoto, Y., Wu, P., Miyoshi, D., Karimata, H. and Sugimoto, N. (2005) DNA-based biosensor for monitoring pH *in vitro* and in living cells. *Biochemistry*, **44**, 7125–7130.